

# Harvard BioRobotics Laboratory Technical Report

December 2000

## **Virtual Fixtures for Robotic Endoscopic Surgery**

Fuji Lai & Robert D. Howe

Division of Engineering and Applied Sciences Harvard University

323 Pierce Hall, 29 Oxford St., Cambridge, MA 02138 USA

PHONE: (617) 496-8359, FAX: (617) 495-9837,

E-MAIL: [howe@deas.harvard.edu](mailto:howe@deas.harvard.edu)

### **ABSTRACT**

This paper describes new computer-assisted technologies to improve efficiency, efficacy, and safety in robot-assisted minimally invasive surgery (MIS). Although these techniques will be applicable to many arenas of robotically-assisted surgery, these methods are expected to have the biggest impact in soft tissue cardiothoracic surgery. We will focus on the coronary artery bypass graft (CABG) procedure where robotic assistance promises significant advantages but current robotic techniques are slow and cumbersome. Our specific aims are to design "virtual fixtures" to assist the surgeon in guiding robotically-aided instruments in teleoperated soft tissue robotic minimally invasive surgery. We also implement these fixtures in a laboratory testbed and assess the performance enhancement from these assistance techniques.

## **INTRODUCTION**

Traditional methods in cardiothoracic surgery have required large incisions such as sternotomies (opening of chest cavity). In contrast, in minimally invasive endoscopic surgery, the entire surgical procedure is carried out using long instruments inserted into the patient's body through small (1cm) incisions with the surgeon manipulating the tool handles from outside the patient's body. There is no direct tactile or visual contact between surgeon and the operative site. Visual feedback is provided by an endoscope, a long tube inserted into the body, which sends back video images. These methods result in reduced patient pain and trauma, fewer complications, and shorter recovery periods.

Although there are several obvious advantages to using endoscopic methods compared to open methods, surgeons face many challenges in making the shift. These include the issues inherent to endoscopic surgery of decreased visual and haptic information, significant motion constraints, and the need for cognitive spatio-motor remapping.

This is where surgical robots come into play. They seek to alleviate some of these human factors issues by increasing the information available to the surgeon while maintaining the minimally invasive nature of the procedure. Robots enhance surgery by improving precision, repeatability, stability, and dexterity. These qualities coupled with the human surgeon's judgment capabilities make a formidable combination.

Control of surgical robots falls into the two basic categories of autonomy and teleoperation (Howe and Matsuoka, 1999). In autonomous systems pre-operative 3-D images are used to plan and execute cutting trajectories for orthopaedic (e.g. hip replacement) and neurosurgery (e.g. tumor resection) applications without further human guidance. However, in soft tissue surgery,

deformation of the tissue is unavoidable, resulting in surgical robots for thoracic and general surgery being used in teleoperation mode thus far. The commercially-available Zeus robotic surgery system (Computer Motion, Inc, Goleta, CA) which we will use in our investigation comprises two instrument positioner robot arms controlled by the surgeon in manual teleoperation mode and a third endoscope positioner arm (Aesop system) which can be voice-controlled. The surgeon has to process sensory information, select a plan of action, and execute the steps. This process is time-consuming and exacts a heavy workload toll on the surgeon.

One of the ways we propose to alleviate these difficulties is through introducing *virtual fixtures*. These are control perceptual overlays that reduce the mental and physical demands of a particular task (Rosenberg, 1993). For instance, in drawing a straight line, human performance is greatly enhanced by using a ruler. This technique is used in many personal computer software applications in the form of "guides" or "snap-to-grid," which makes the mouse move along straight lines despite small excursions of the mouse. Similarly, a virtual fixture could be added to the surgical robot controller to help guide the surgeon in making a straight incision. By incorporating the robot's ability to use 3-D image data, the virtual fixture can help the surgeon locate particular tissue structures, or to dissect near a structure while enforcing a safety margin to prevent injury to the structure itself. This is a good illustration of the safety benefits of using virtual fixtures.

A natural progression from the virtual fixtures would be *surgical macros*. Macros are surgical subroutines invoked by the surgeon to assist in completing surgical tasks. A surgical macro is a sequence of commands that the robot executes autonomously. A feature of a surgical robotic system is that we have detailed position information of instrument tips. Thus if we give

the robot some knowledge of the surgical environment we are able to safely drive the surgical instruments to the desired position to carry out parts of procedures autonomously.

This project will focus on the robotically-assisted CABG procedure. The CABG is a good candidate procedure with which to demonstrate the efficacy and widespread applicability of our developed techniques due to the relatively fixed nature of the tissue structures. This procedure has been successfully performed completely endoscopically using robots and not only serves as a benchmark procedure but is a procedure that stands to benefit greatly from computed robotic assistance. Coronary artery disease is the single leading mortality cause in the U.S. and the coronary artery bypass graft is the most common surgical procedure performed with more than 750,000 cases per year worldwide. In this procedure the internal mammary artery is mobilized from the chest wall to bypass an occluded section of artery and provide a new blood supply for the heart. Approximately 10 cm of the IMA is blunt-dissected free, using a harmonic scalpel or electrocautery. This process is called 'IMA harvest' or 'takedown.' Each major branch must be located and sealed using meal clips or cauterization to prevent significant blood loss, while avoiding damage to the artery itself. In the minimally invasive case, this is a laborious process that can take up the majority of the procedure since the robotic system allows limited dexterity as well as reduced visibility and haptic information. Observed trials with the Zeus robotic system required about 70-120 minutes for IMA harvest, about 75% of the total time. Methods for speeding up the branch localization and dissection processes would greatly decrease surgery time and reduce the sensory and control demands on the surgeon. Since the IMA is firmly attached to the chest wall, its location is relatively stable with respect to anatomical landmarks. Thus we can use preoperative 3-D CT images of the surgical site to guide the instruments. While the idea of autonomous soft tissue surgery has intrigued some as an interesting research challenge, the idea

has not been examined in detail by developers of commercial surgical robots due to the practical complexity involved in developing an autonomous system applicable in common to most surgery procedures.

A significant contribution of this project is that we will enhance control of robot surgery systems. We will develop new fundamental, computer-aided techniques that will form a foundation for intelligent soft-tissue robotic surgery. We hypothesize that these aids will improve performance and safety as well as surgeon workload. These techniques will not be unique to the specific robotic system used in the investigation. These methods will also be widely applicable to various forms of surgery. Our research seeks to bridge the transition between conventional teleoperated modes of soft tissue robotic surgery and as we foresee, the eventual, widely-available, practical implementation of autonomous soft tissue robotic surgery.

Also, in developing these computer aids we will address basic issues of human-machine interaction. We will learn about control sharing (supervisory) and control trading (autonomous) between human and robot. We will learn which parts of tasks can be delegated to the computer and which parts still need the indispensable talents of the human surgeon. We will arrive at an understanding of the information transfer processes (cognitive, haptic, motor) involved in carrying out a mentally and physically challenging task such as a surgical task.

## **METHODS**

### **Experimental Setup**

We implemented the virtual fixtures on a tabletop teleoperated system using two PHANTOM® haptic devices (Sensable Technologies, Cambridge, MA) (Debus, 1999). Both devices are the

classic 1.5 model, as shown in Figure 1. Each device is a 6 degree of freedom manipulator. The first three joints are cable driven which creates a very low friction mechanism and are used to actuate the robot's tip. Attached to the robot's tip is a passive spherical wrist that provides the three remaining degrees of freedom. The position of each joint is known through the use of high resolution optical encoders. The operator controls the master by manipulating a stylus attached through a passive spherical wrist. The workspace is roughly a box of dimension 19 cm  $\times$  27 cm  $\times$  38 cm. Each device can exert a continuous tip force of 1.7 N, and a maximum force of 8.5 N can be achieved.

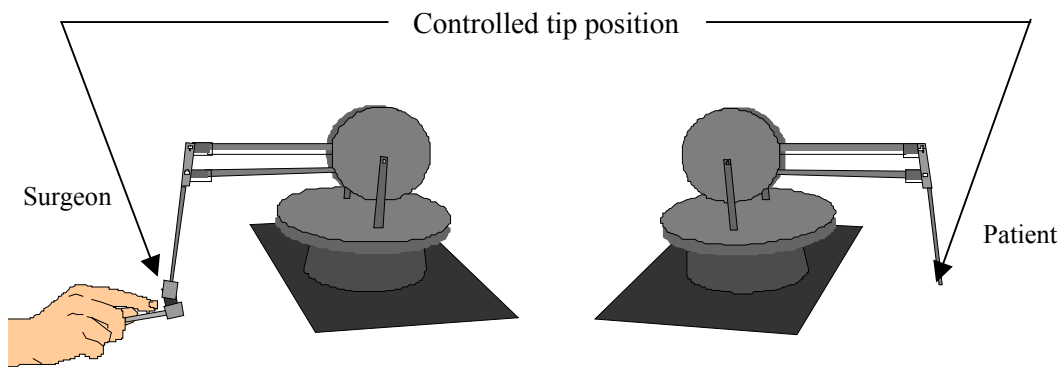


**Fig. 1:** Teleoperated setup

The computer hardware structure used to read the encoders and control the motors includes an interface card and a power amplifier. The system software includes a BASIC/IO subroutine library that contains all the drivers and functions necessary to command the system. Among all the functions already programmed for the device, two useful functions are the forward kinematics and inverse dynamics. The forward kinematics function provides the position and orientation of the robot's tip in the base frame. The inverse dynamics function allows control of

the robot through the use of Cartesian force vector as input. These functions can be easily called from a C program.

In order to control the teleoperation system, a symmetric proportional control scheme based on position and velocity errors between the master and remote manipulators is employed. In this control method, position and velocity of the master robot are used as position and velocity commands to the remote robot. Similarly, the position and velocity of the remote robot are used to compute feedback forces applied to the master robot.

$$\begin{aligned}
 F_i^{remote} &= K_{pi} \mathbf{d}_i^{master} - X_i^{remote} \mathbf{i} + K_{vi} \mathbf{d}_i^{master} - \dot{X}_i^{remote} \mathbf{i} \\
 F_i^{master} &= -F_i^{remote}, \quad i = \mathbf{l}_{x,y,z} \mathbf{q}
 \end{aligned} \tag{1}$$

where  $X_i, \dot{X}_i$  and  $F_i$  are the  $i^{\text{th}}$  components of the tip position, velocity and force, and  $K_{pi}$  and  $K_{vi}$  are the proportional and derivative gain components. In implementing our fixtures we added constraints to the movement of the remote manipulator by having the remote manipulator follow the position of a virtual projected position computed to reflect the added virtual constraints.

### **Incision Fixture**

The first aid we will develop is the simple straight-line virtual fixture to aid in incision-making. This is the simplest aid to begin our investigation with. One point to note is that all our applications will be position-based, without the incorporation of force feedback. This fixture would have the surgeon specify with the robot instrument tip start point and end point of the incision as well as a third point on the intervening tissue. The surgeon would specify a desired incision depth as well. The registration of the three points allows the robot controller to compute the equation of the incision line in space as well as the equation for the tissue plane. The robot controller would then help keep the cutting tool centered along the line as the surgeon makes the

incision. The virtual fixture would work by confining the responsiveness of the slave instrument tip positioning to the desired incision region. The slave instrument is free to follow the master instrument when in the region outside the tissue but is confined to the incision plane when the instrument tries to enter the tissue. In the instance whereby the master is in a position corresponding to a position in the tissue but outside the incision region, the slave is mapped to the incision plane and the closest point within that region. Thus, in a similar manner to a snap-to-grid concept in using a computer mouse, the output is limited to a precisely straight-line incision, regardless of small deviations of the surgeon's executed input from the desired line.

### ***Design of incision fixture***

Three points are specified by the surgeon (P1,P2,P3) as well as incision depth. P1, P2, P3 define the tissue plane and P1 and P2 define the incision line.

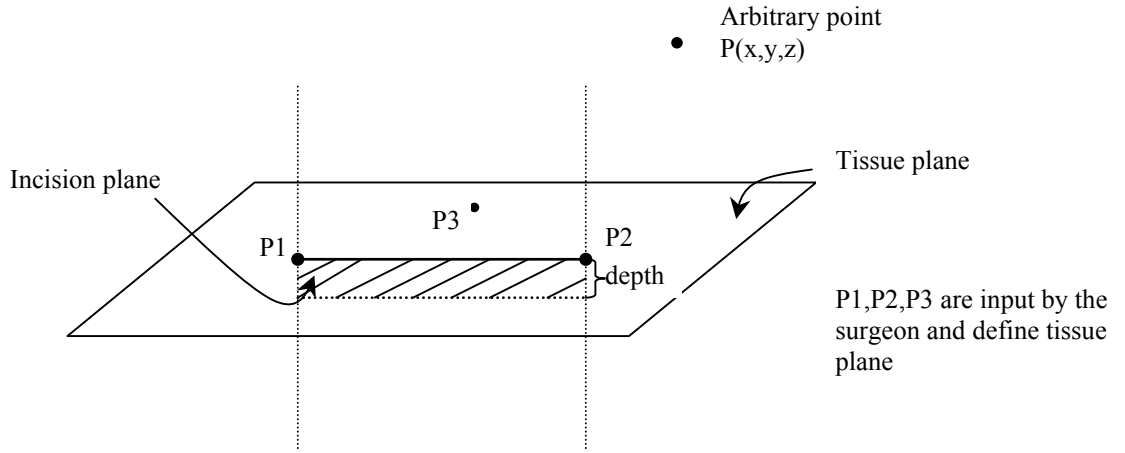


**Fig. 2: 3D diagram of points and plane definition**

Incision line:  $\mathbf{p}_1 + t(\mathbf{p}_2 - \mathbf{p}_1)$  where  $0 < t < 1$

Tissue plane:  $ax + by + cz + d = 0$  where  $a = y_2z_3 - z_2y_3$  notation:  $x_{21} = x_2 - x_1$   
 $b = z_2x_3 - x_2z_3$   
 $c = x_2y_3 - y_2x_3$   
 $d = -(x_2a + y_2b + z_2c)$   
 $m = \text{magnitude} = \sqrt{a^2 + b^2 + c^2}$

Unit normal to tissue plane:  $\mathbf{n}_t = n_1\mathbf{i} + n_2\mathbf{j} + n_3\mathbf{k}$  where  $n_1 = a/m$ ;  $n_2 = b/m$ ;  $n_3 = c/m$

Distance from tissue plane:  $r^2 = \frac{(ax + by + cz + d)^2}{a^2 + b^2 + c^2}$

Incision plane:  $\mathbf{p}_4 = \mathbf{p}_1 + (a\mathbf{i} + b\mathbf{j} + c\mathbf{k})$  where  $\mathbf{p}_4$  is an arbitrary point on the incision plane;  
 using points P1, P2, P4 we can define the incision plane as,  
 $a_1x + b_1y + c_1z + d_1 = 0$

Unit normal to incision plane:  $\mathbf{n}_i = n_4\mathbf{i} + n_5\mathbf{j} + n_6\mathbf{k}$

Distance from incision plane:  $r_1 = \frac{(a_1x + b_1y + c_1z + d_1)^2}{a_1^2 + b_1^2 + c_1^2}$

Projected onto incision plane:

Projection is defined as:  $\mathbf{p} - \mathbf{n}_i r_1$

Regions of motion shown below:

- I: free to move within projected point on incision plane
- II: projected onto closest point on line segment fg (point where normal strikes line between segment end points; otherwise it is nearest segment end point)
- III: projected onto line ef
- IV: projected onto line gh
- V: projected onto corner point f
- VI: projected onto corner point g

To find projection of point J onto line segment KL:

$$x = x_K + t(x_L - x_K) \text{ where } 0 < t < 1$$

$$y = y_K + t(y_L - y_K) \text{ where } 0 < t < 1$$

$$z = z_K + t(z_L - z_K) \text{ where } 0 < t < 1$$

$$\text{where } t = \frac{[(x_K - x_J)(x_L - x_K) + (y_K - y_J)(y_L - y_K) + (z_K - z_J)(z_L - z_K)]}{(x_L - x_K)^2 + (y_L - y_K)^2 + (z_L - z_K)^2}$$

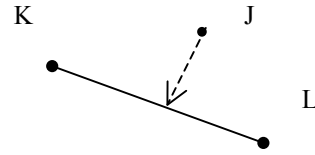


**Fig. 3: Projection of a point onto line segment**

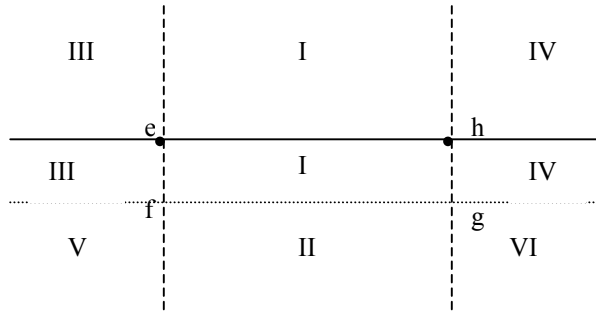


**Fig. 4: Side view of incision plane and regions of projection**

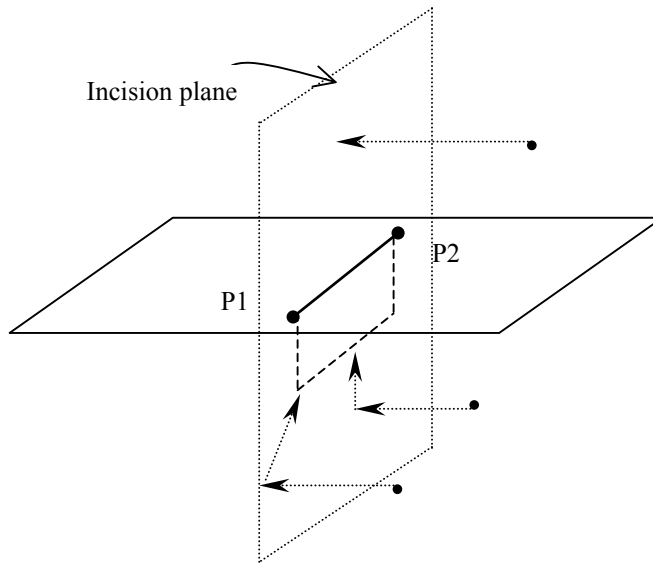


**Fig. 5: 3D view of fixture and projection sequence**

### ***Performance Evaluation of Incision fixture***

It is evident from the spatial trajectories that the remote manipulator is confined to the precise desired incision. Also, by measuring the parameters from the plots we have checked the accuracy of the dimensions of the incision made.

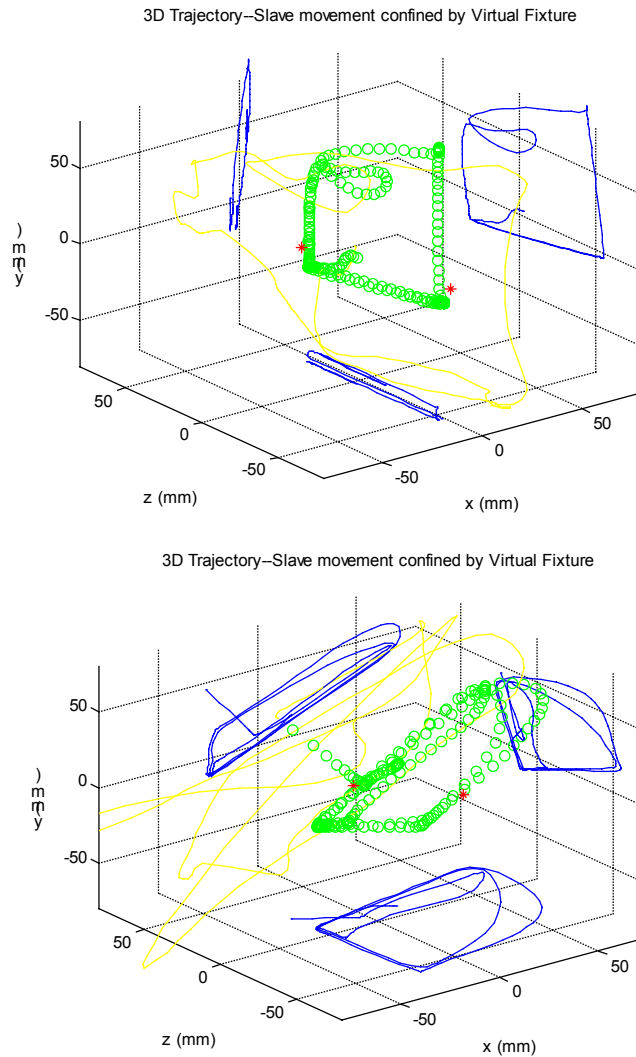


**Fig. 6: Spatial trajectories of master and corresponding slave movements and projections onto x,y,z planes—a) incision length 7cm, depth 2cm; b) incision length 6cm, depth 3cm (master=yellow; slave=green; plane projections=dark blue)**

We can gauge the effectiveness of the fixture by comparing trajectories of tasks carried out with and without the incision fixture. We can quantify the difference by measuring the rms (root-mean-square) deviation of the non-aided case. There are several different directions of deviation we can measure. They are:

- i) deviation from incision plane

- ii) deviation outside at start boundary of incision line
- iii) deviation outside at boundary of incision line
- iv) deviation deeper from depth boundary of incision

### ***Experimental Protocol***

The fixture was assessed by carrying out simulated incision trials with and without the aid of the virtual fixture. Five subjects, all right-handed, were recruited for these experiments. The set up consisted of a simulated incision-making situation. The subjects were seated in front of a TV monitor feeding back a video image of the remote operative site. They were instructed to hold on to the stylus of the Phantom. The task given to them was to execute a straight line incision 1 cm in depth between the given left start and right end markers on the simulated tissue. The distance between the markers was 5 cm. They were instructed to perform the incision as accurately as possible and as decisively as possible. The positions of the markers and tissue plane were registered by contacting the marker points and a third intervening point on the tissue plane. The subjects were allowed some time before recording of data to become comfortable with the interface and the task. Each subject completed the task ten times. Five of those were with the aid of the fixture and five without the aid of the fixture. These were presented in random order to minimize the effect of learning on the comparison of the two cases. The performance measures were the rms errors in each of the four directions as described previously.

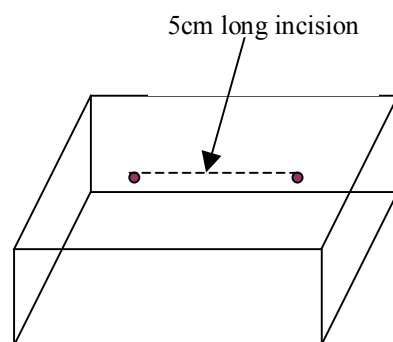


**Fig. 7: Setup of incision experiment**

The effect of the fixture on task performance is summarized in the figure below. The rms value types are defined as i) error with respect to incision plane; ii) error at start point; iii) error at end point; iv) error with respect to desired maximum depth (including undercutting as well);

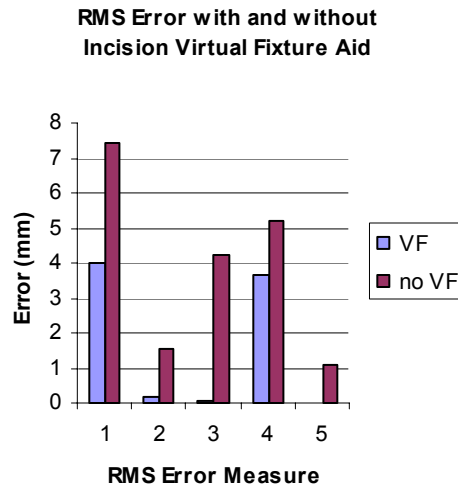


**Fig. 8: Comparison of performance with and without virtual aid**

v) error with respect to desired maximum depth (overcutting only). Analysis of variance showed that the p-values for the comparison of these errors with and without the incision fixture aid were 0.01, 0.04, 0.000005, 0.02, 0.01 respectively. This gives evidence of statistical significance of performance and safety improvement with the incision fixture.

### **Dissection Fixture**

This fixture involves development of image-guided techniques. Since the IMA is a relatively fixed structure, we are able to use pre-operative image-guided methods to speed up the IMA harvest portion of the CABG procedure. We can imagine the surgery proceeding as follows. Prior to surgery three metal pins will be inserted percutaneously into the patient's ribs to act as

fixed reference fiducial markers. The patient will then undergo CT scanning. During the scan a contrast agent will be injected into the mammary artery to visualize the location of the artery. The resulting image set will be segmented to define the location of the artery relative to the registration pins, and the location of each major branch of the artery will be determined. The surgeon will then register the pins in the robot frame by bringing the tip of a robot-mounted calibration instrument into contact with each of the pins. Thus the robot can determine the location of the artery in robot coordinate frame.

The fixture would work as follows. Now that the robot has awareness of position of the artery, it can thus move directly to the location of each artery branch and seal it using cautery or clips (Fig. 9) without the need for the surgeon to painstakingly dissect adjacent to the artery to expose the branch. After the arterial branches have been isolated, the robot controller will create a virtual fixture surrounding the artery as a safety envelope. This fixture will guide the surgeon during dissection by adding a safety margin as well as varying gains of master-to-slave movement depending on the proximity of the artery to the region in which the instrument tip is working (Fig. 10). This means that an input movement is scaled up or down depending on how close the instrument tip is to the region of the artery. At a very close distance to the artery, within the safety envelope, the slave instrument tip will not respond to movements of the input device that would endanger the artery. Whereas, at a distance away from the artery, the scale of master-slave motion will be increased as less precision is needed. This fixture will decrease the precision required of the surgeon and will increase safety by reducing risk of inadvertent injury to the artery itself.

A progression from the virtual fixture would be to have an IMA harvest macro. Since the controller has awareness of the position of the IMA, the robot can drive the instruments to lay

“tracks” on either side of the artery at a safe distance away from the artery. After the tracks are laid, the surgeon can come in and concentrate his/her efforts on the designated region of tissue. We can foresee several variations of this macro which incorporate varying levels of autonomy.

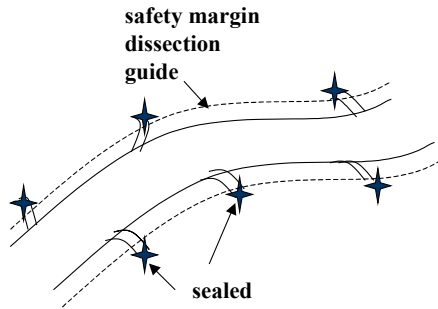


**Fig. 9: Safety margin envelope to protect vulnerable region**

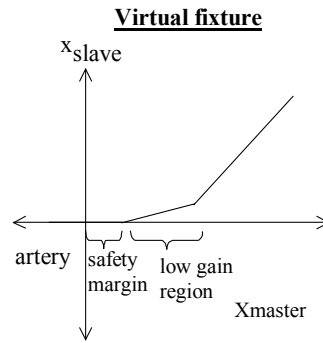


**Fig. 10: Positioning profile of virtual fixture for safety margin**

***Design of Plane Dissection fixture***

In the dissection fixture three points P1,P2,P3 are defined as well by the surgeon. This allows us to compute the danger plane similarly as the incision plane was calculated in the incision fixture. This plane serves as a safeguard as the distance of the instrument from this plane results in varying gains of the movement of the slave instrument tip.

Gain profiles for blunt dissection fixture:

First gain profile allows gain of 1 until safety boundary is reached and then motions are scaled down in order to allow greater precision and safeguard against entering too far into the danger region. The gain falls off exponentially as the instrument ventures further into the danger zone. The features of the exponential can be adjusted by the surgeon.

The second gain profile does not allow any movement at all into the danger region. As the instrument moves away from the danger zone gain ramps up to one. The features of the exponential function can be input by the surgeon.

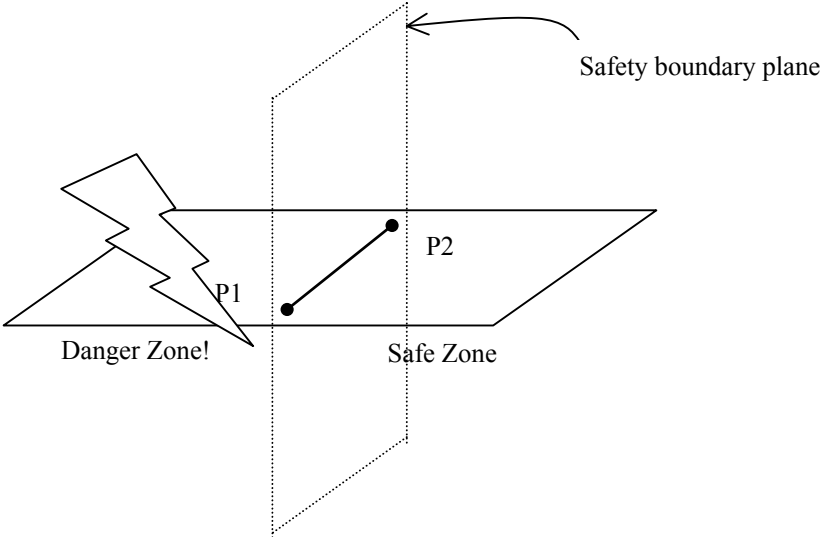


**Fig. 11: 3D view of safety margin concept**

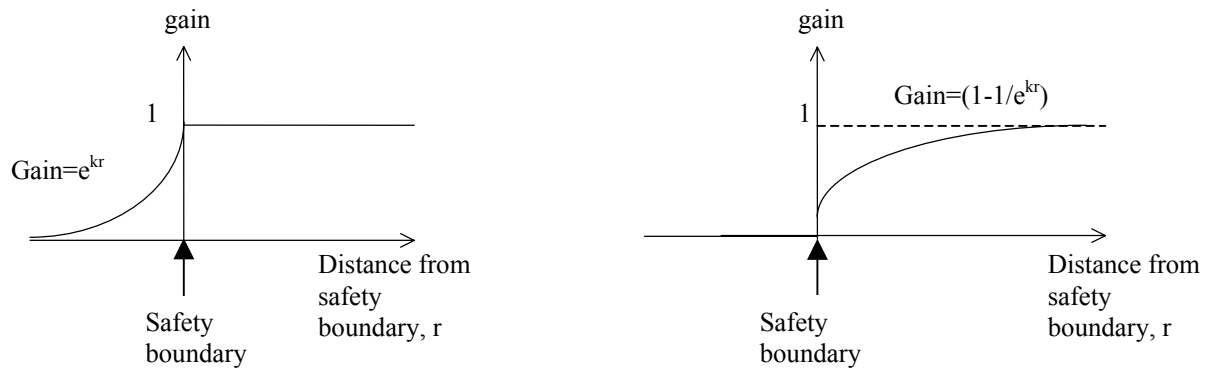
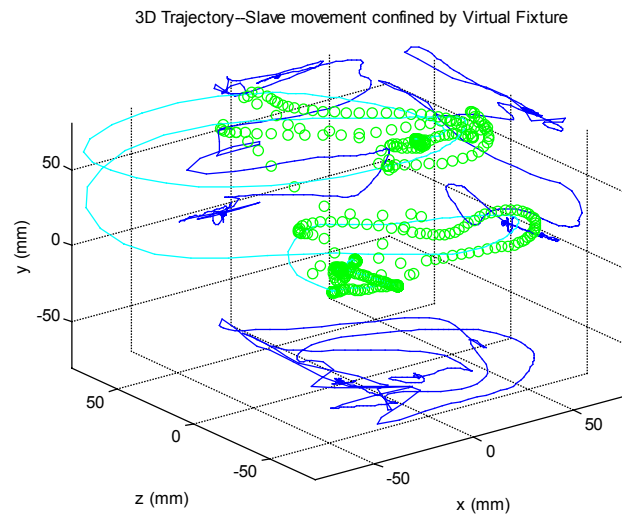


**Fig. 12: Gain profiles for blunt dissection fixture—**a) exponential decrease in danger region; b) exponential rise to 1 in safe region

### *Performance Evaluation of Plane Dissection fixture*

From the figures it is evident that the fixture has safeguarded the vulnerable region by scaling down movements in that region (safety boundary plane is yz plane at  $x=0$ ). Movements in the



negative x region are dramatically limited in Fig. 13 (a), (b) while completely eliminated in (c).

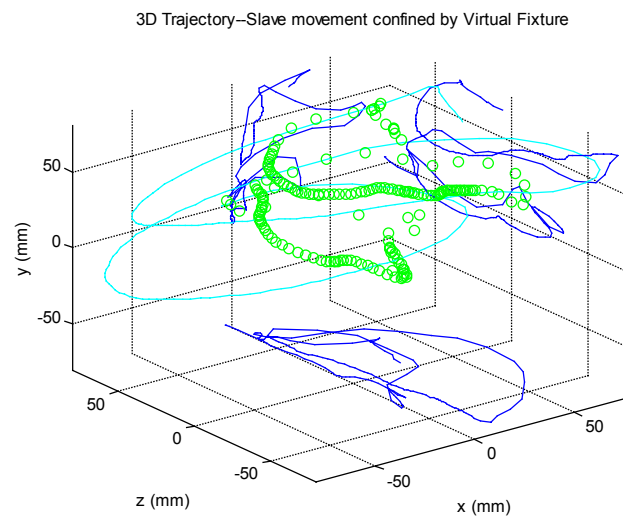
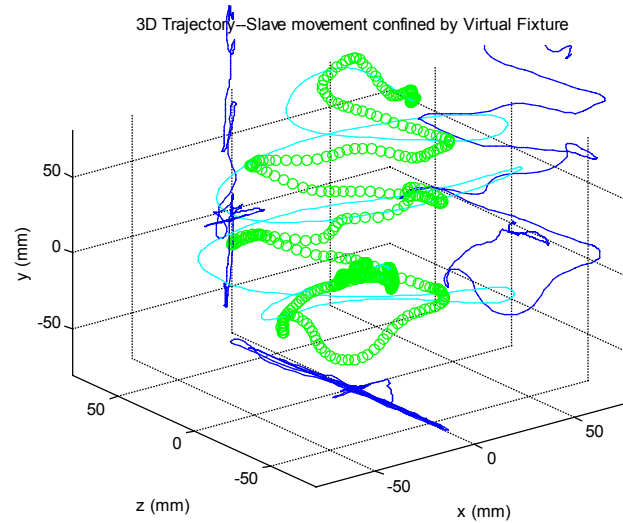


**Fig. 13: Spatial trajectories of master and corresponding slave movements and projections onto x,y,z planes-(a) & (b) from Fixture A; (c) from Fixture B (master=light blue; slave=green; plane projections=dark blue)**

### ***Design of Cylindrical Dissection fixture***

This 3D envelope can be used to safeguard the vessel. Once the position of the vessel is known from pre-operative imaging, we can design a safety envelope around the vessel so that the remote manipulator (instrument tip) is not allowed to approach the vessel any closer than

specified by the safety thickness margin. Any master movements to points within the envelope are mapped to the closest point on the envelope. A straight cylindrical envelope is used in our setup but this concept can easily be extended for a curved section as well by using incremental cylinders registered to the vessel positions obtained from the preoperative CT images.

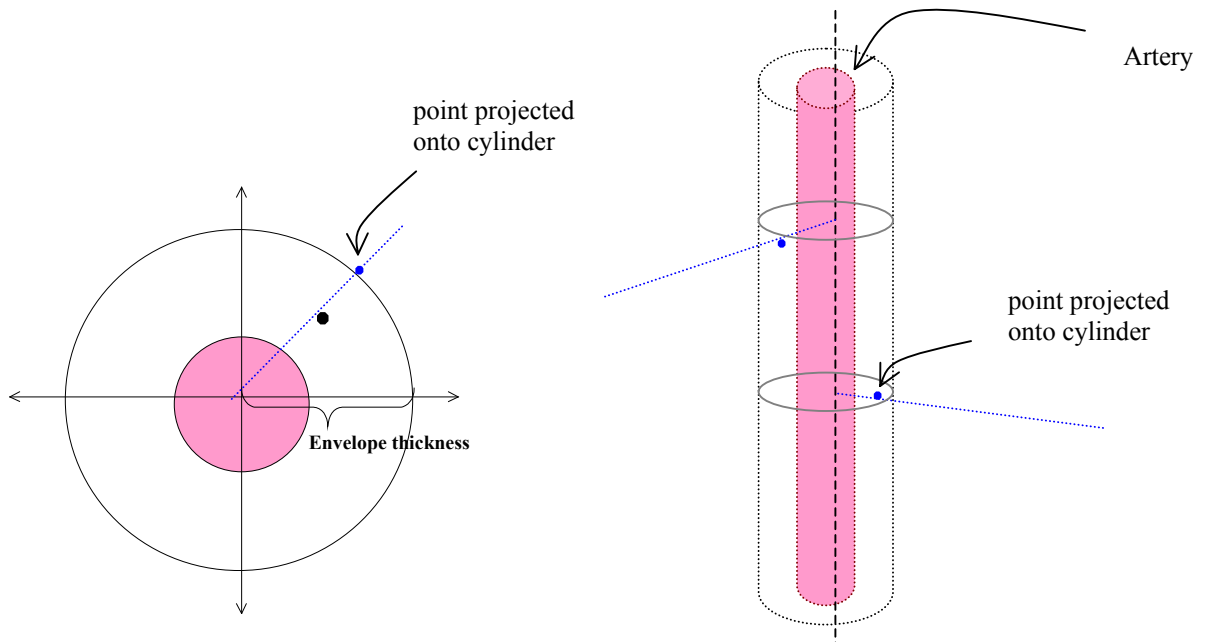


**Fig. 14: Design of Safety Cylinder for Dissection—**a) Cross-sectional view of artery and fixture; b) side view of artery and fixture

The algorithm involves:

Finding the projection of the point into line of artery

Find distance of point from line

If distance of point from line < safety margin, project the point onto the closest point on the cylinder.

### ***Performance evaluation of cylindrical dissection fixture***

It can be seen that the envelope safeguards the vessel by preventing the dissection tool from entering the envelope region. In the first figure the artery can be imagined as running from top to bottom as seen on the plot. Therefore the remote instrument movements can be seen to be restricted from entering the artery region. This is evident from the projection onto the xz plane. In the second figure the artery can be imagined as running from left to right and the remote instrument movements are seen to be restricted from entering the cylindrical region of the artery.

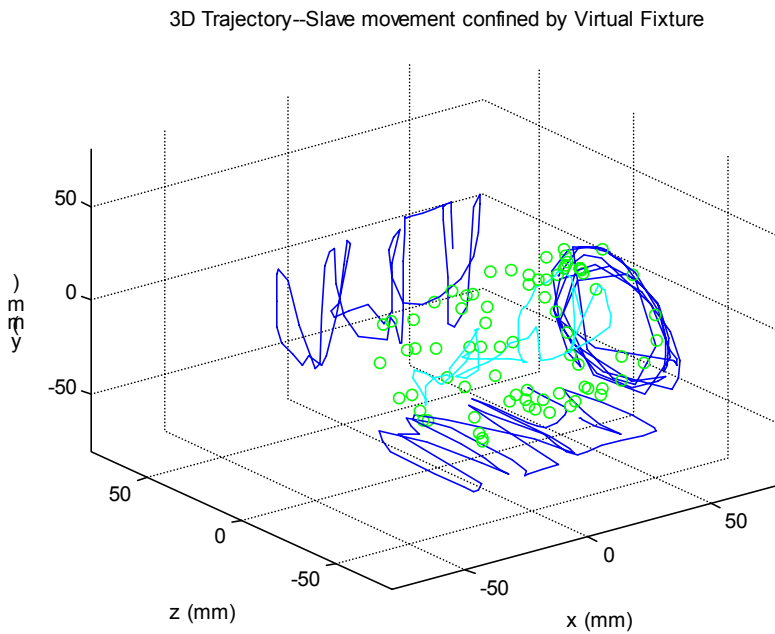
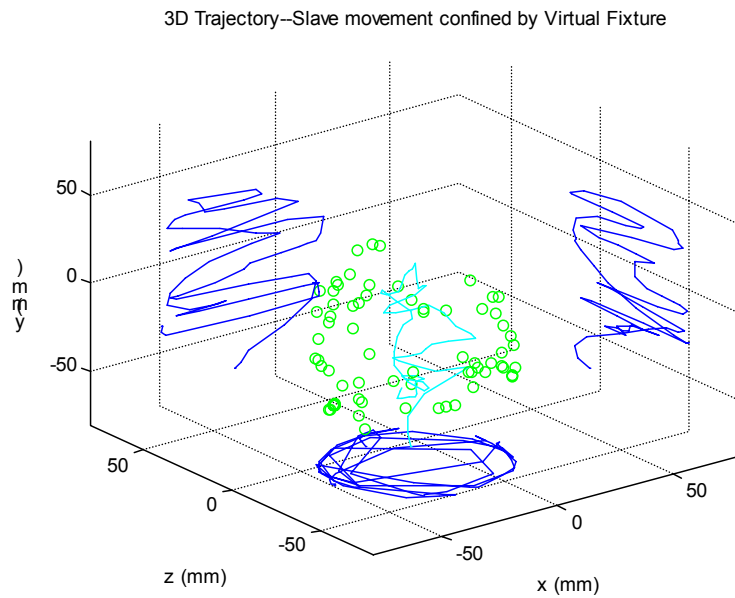


**Fig. 15: Performance evaluation of safety envelope for dissection (master=light blue; slave=green; plane projections=dark blue)**

*Experimental Protocol*

To assess the performance benefits of using a fixture such as the cylindrical fixture in blunt dissection, we carried out simulated trials. We enlisted five subjects, all right-handed, for these experiments. The task of blunt dissection was simulated by placing a thin cylindrical deformable tube within a block of soft material simulating tissue. The subjects were instructed to dissect out a colored segment 5 cm long on the tube such that the entire colored section was visible. They were instructed to perform the task as efficiently as possible but while maintaining the safety of the vessel. The position of the tube was registered by contacting the ends of the tube before starting the trial. This allowed computation of any excursion of the dissection tool into the vulnerable region of the vessel. Each subject was exposed to this task a total of three times for each experimental condition, with and without fixture. The trials were randomized. The experimental setup is shown below. The performance measures noted were time to completion and also rms error or excursion into the vessel region.

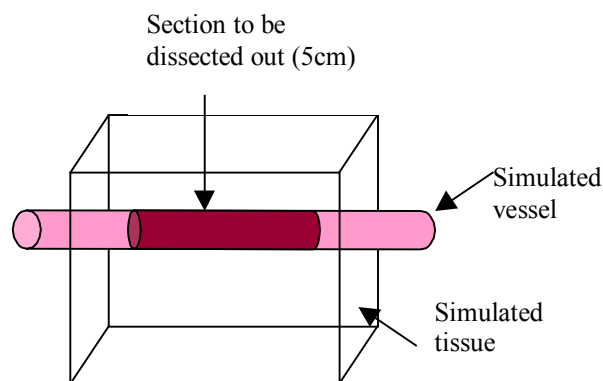


**Fig. 16: Experimental setup with simulated blunt dissection of vessel**

The results are summarized in Fig. 17. It can be seen that the virtual fixture did indeed result in lower rms error, emphasizing the safety benefits of using the fixture. The analysis of variance

showed definite statistical significance for the performance benefits of using the fixture, with a p value of 0.00002.

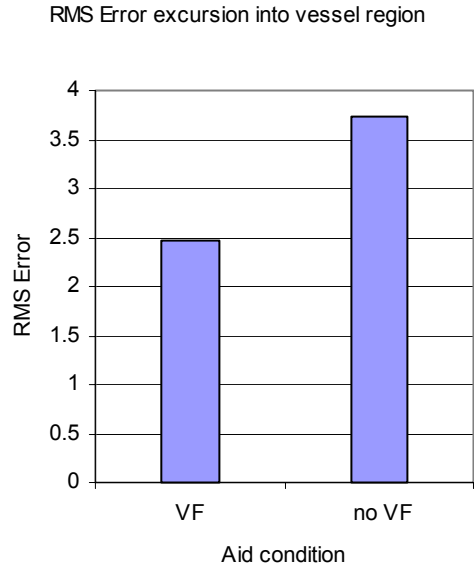


**Fig. 17: Comparison of performance with and without dissection fixture**

## **CONCLUSIONS AND FURTHER THOUGHTS**

This project involved design, implementation, and evaluation of virtual fixtures as aids for surgical tasks. We have successfully completed all the objectives, proven the concept, and have been able to showcase the use of virtual fixtures for surgery as a shining example of collaborative teleoperated control. This laboratory testbed study has confirmed the effectiveness of the concept and design. This study opens the way for clinical implementation of these concepts in the near future.

## **REFERENCES**

Debus, T (1999), “Automatic identification of local geometric properties during teleoperation.”

Masters thesis. Boston University.

R.D.Howe and Y. Matsuoka (1999), "Robotics for surgery," *Ann. Rev. Biomed. Eng.* **1**:211-240.

Rosenberg, L.B. (1993). Virtual fixtures: Perceptual tools for telerobotic manipulation. In:

*Proceedings of the IEEE Virtual Reality Annual Intl Symposium*, pp. 76-82.